Limnol. Oceanogr., 51(6), 2006, 2632–2645

Hydrodynamic control of the underwater light climate in fluvial Lac Saint-Pierre

Jean-Jacques Frenette
Université du Québec à Trois-Rivières, Département de Chimie-Biologie, C.P. 500, Trois-Rivières, Québec G9A 5H7, Canada

Michael T. Arts
National Water Research Institute, Environment Canada, 867 Lakeshore Road, P.O. Box 5050, Burlington, Ontario L7R 4A6, Canada

Jean Morin
Environment Canada, Meteorological Service of Canada, 1141 rte de l'Eglise, Sainte-Foy, Québec G1V 4H5, Canada

Denis Gratton and Carl Martin
Université du Québec à Trois-Rivières, Département de Chimie-Biologie, C.P. 500, Trois-Rivières, Québec G9A 5H7, Canada

Abstract

We measured characteristics of the underwater light spectra (e.g., attenuation of ultraviolet [UV] radiation, photosynthetically active radiation) and select dissolved and particulate physicochemical properties (e.g., chromophoric dissolved organic carbon [CDOM], dissolved and particulate organic carbon, inorganic dry weights, beam attenuation coefficients, particulate absorption coefficients, and nutrients) in different water masses of fluvial Lac Saint-Pierre (Canada). We used these variables as tracers to reveal the extent and magnitude of spatial and temporal heterogeneity in this large, shallow, fluvial lake of the St. Lawrence River. We superimposed these tracer variables over radiance data obtained from satellite images to identify spatial and temporal changes in the distribution of different water masses and their bio-optical components. The underwater light environment showed strong horizontal (longitudinal and lateral) variability because of the strong connectivity between the terrestrial and aquatic environments in the lake's tributaries and adjoining wetlands. Analyzing the downstream distribution of optical and chemical variables as a function of transport time rather than distance from source tributaries allowed us to demonstrate large differences in the age of the different water masses depending on the characteristics of the source tributary, in-stream processes, and distance from its source. CDOM explained most of the UV attenuation and allowed the greatest discrimination between water masses.

Nature is organized along three spatial dimensions, a fact which contributes to its complexity. Traditionally the physical, chemical, and biological processes occurring within lake ecosystems have been described mostly in two dimensions, that is, with emphasis on bivariate combinations of physical, chemical, and biological variables over time, but especially with depth. Such variables include changes in light attenuation and vertical distributions of plankton and predators, factors that are strongly influenced by stratification (epi-, meta-, and hypolimnion), mixing regimes within the water column, or both.

This approach has been applied successfully to the pelagic zone of lakes on the basis that this area is the most representative portion of the lake (in volume), despite the pre-eminent importance of the littoral zone in terms of productivity (Wetzel 2001). This might, in part, explain why shallow littoral stations are typically undersampled compared with deep stations, even though they are the most productive regions in lakes. Littoral zones are also the sites of terrestrial influxes of nutrients and of light-attenuating organic and inorganic matter, resulting in large differences in underwater light climate between inshore and offshore regions of lakes (Frenette and Vincent 2003). This horizontal (i.e., inshore–offshore) heterogeneity is further accentuated in fluvial lakes (especially in fluvial lakes with multiple inflows), which can result in the formation of chemically and therefore spectrally distinct water masses within the lake (Frenette et al. 2003). In fluvial lakes with large width/depth ratios, such water masses often persist and can exhibit reduced lateral mixing downstream (Frenette et al. 2003), conferring a unique pattern of

Acknowledgments

We thank Christine Barnard, Pierre-André Bordeleau, Olivier Champoux, Kim Huggins, Marianne Lefebvre, Marie-Audrey Livernoche, Sylvain Thélème, and Geneviève Trudel for their invaluable help in the field and in the lab. We thank captain Guy Morin of the ship *Le Pêcheur* of the Meteorological Service of Canada, Environment Canada, and captain Roger Gladu for sharing their experience and knowledge of Lac Saint-Pierre. Warwick Vincent critically reviewed this manuscript.

This research was funded by the Natural Sciences Research Council of Canada (NSERC) and the Fonds Québéquois de la Recherche sur la Nature et les Technologies (FQRNT) to J.-J.F.; National Water Research Institute (NWRI), Environment Canada to M.T.A.; and Meteorological Service of Canada to J.M.

This study is a contribution of the Groupe de Recherche Interuniversitaire en Limnologie (GRIL).

primarily horizontal, rather than vertical, stratification (as in deep lakes).

Deep-water zones of lakes are generally much less affected by nearshore macrophytes or wind-driven particle resuspension from the bottom. In contrast, fluvial lakes are generally characterized by a relatively large biomass of submerged macrophytes and could also be affected by wind-induced mixing regimes that can further modify characteristics of their internal water masses through sediment resuspension (Scheffer 1998). Despite such observations, water quality monitoring strategies in fluvial lakes, and in other lake types, typically emphasize sampling at offshore sites even though these are not the primary sites of water quality problems (Frenette and Vincent 2003).

Lotic ecosystems are characterized by strong, multidimensional environmental gradients. These spatial and temporal gradients directly affect key ecological processes ultimately translating into strong effects on biodiversity, productivity (Wiens 2002), and stability (Huxel and McCann 1998). For example, rapid expansion and contraction in water levels (river discharge) has a major influence on the degree of *connectivity* (i.e., magnitude and direction of exchanges of energy, matter, and organisms) among habitats (Tockner et al. 2000). Longitudinal, downstream patterns in habitat variables of rivers has served as a central theme in lotic ecology, but much less attention has been given to the lateral dimension (Ward and Tockner 2001). Recent studies have shown that lateral transfers of materials between habitats can have strong effects on organisms, ultimately affecting the stability and resilience of ecosystems (Huxel and McCann 1998).

Physical and chemical variables (e.g., NO_3, specific conductance, shoreline index, etc.) have been used to characterize the degree of connectivity or spatial heterogeneity between habitats (Poole 2002). However, the degree of connectivity among habitats should also be strongly influenced by the underwater light regime. Underwater light climate has many documented, pivotal roles in photochemistry and photobiology—for example, affecting the production of labile dissolved organic matter, controlling primary productivity, affecting vision and behavior of adult and larval fish, and affecting many other processes. Underwater spectral composition of light can operate in subtle but nonetheless consequential ways, for example, by modifying lipid composition and algal stoichiometry which, in turn, has implications for food quality and nutrient transfers to higher trophic levels (Rai et al. 1997; Frenette et al. 1998; Sterner and Elser 2002).

Complexity in fluvial lakes is further enhanced by differences in current velocity (transport time) among water masses. Transport time within each of the water masses is affected by discharge of individual tributaries, friction generated by macrophytes, proximity to shore, and river bed morphology (Morin et al. 2000*a*). These differences in transport time interact with chemical characteristics of the different water masses to produce heterogeneity in underwater spectral quantity and quality.

We measured characteristics of the underwater light spectra along with selected dissolved and particulate variables in the different water masses of Lac Saint-Pierre to reveal the extent and magnitude of spatial and temporal variability in this large and hydrodynamically complex fluvial lake. These data were compared with radiance data obtained from satellite sensors—Landsat-ETM (Enhanced Thematic Mapper) and Terra-ASTER (Advanced Spaceborne Thermal Emission and Reflection Radiometer)—to identify spatial and temporal changes in water mass distribution and their bio-optical components. Downstream changes in bio-optical and chemical signals were examined by relating these variables to downstream transport time with two-dimensional hydrodynamic simulations for spatial integration instead of the more usual method of expressing variables as a function of the linear distance from incoming tributaries. This is a more realistic way to portray underwater light (ultraviolet [UV]) attenuation.

Methods

Study site—Lac Saint-Pierre (46°12′N; 72°50′E) is the largest (~400 km²) fluvial lake along the St. Lawrence River and the last major enlargement (13.1 km width at mean discharge) of the river before the St. Lawrence Estuary. Lac Saint-Pierre is shallow (mean depth of 3.17 m during the period of mean discharge) and is covered with extensive macrophyte beds during summer. Its large width/depth ratio at least initially reduces lateral mixing between the lake's water masses (Frenette et al. 1989, 2003).

We visited between 25 and 30 sampling stations in 2001 situated along three north–south transects located perpendicular to the main east–west axis of Lac Saint-Pierre (roughly nine stations per transect) on 08 and 27 June, 18 July, and 13 August (Fig. 1a–d). The exact station locations were fixed by a digital Global Positioning System with ±2 m accuracy.

Satellite analysis for identifying the main water masses of Lac Saint-Pierre—The color-producing agents responsible for the color of inland waters can be separated into two groups: chromophoric dissolved organic matter (CDOM) and suspended particulate inorganic matter. Optical satellite sensors allow these elements to be quantified from space (Jerome et al. 1994; Bukata et al. 1997).

We used Landsat (ETM) and Terra (ASTER) satellite images of Lac Saint-Pierre to identify where stations were located within each water mass during each sampling period (Fig. 1; Table 1). To take advantage of the color-producing agent approach for the mapping of Lac Saint Pierre water masses, we had to confirm the contribution of the green (520–600 nm) and red (630–690 nm) bands on the available satellite images. An analysis of the spectral response with the ratio of red to green surface reflection along transects from north to south in Lac Saint Pierre showed that the northern water mass has a higher red/green ratio than the central water mass, which in turn also has a lower ratio than the southern water mass. The main difference between the northern and southern waters is the red reflection, which is significantly more important than the green. The mapping approach used a combination of digital unsupervised classification and image enhancement techniques to manually delineate the different water masses

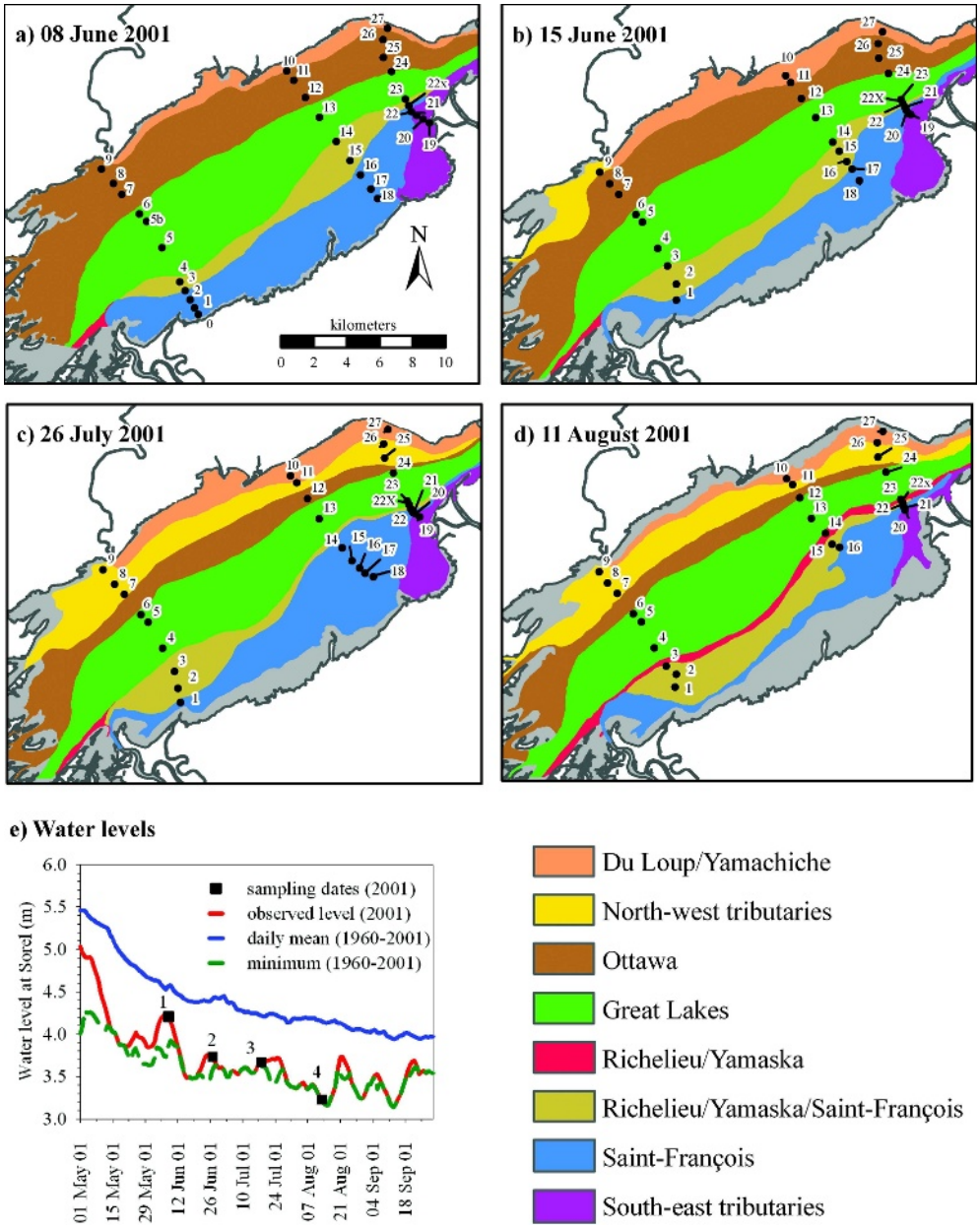

Fig. 1. (a–d) Locations of the sampling stations in relation to the distribution of water masses. (e) Water levels in Lac Saint-Pierre in 2001.

(Bruton et al. 1988). The 15 June and 26 July Terra ASTER images were used to characterize the station positions relative to each water mass for the 27 June and 18 July in situ sampling campaign, respectively. Although these two sampling dates did not coincide with dates for which cloud-free satellite images were available, the absence of dramatic changes in water level during this period (Fig. 1, inset) justifies this decision. Landsat ETM images taken on 08 June and 11August were used for the 08 June and 13 August sampling campaigns, respectively.

With both ETM and ASTER images, the mapping process focused on regrouping spectral values with the use of, on one hand, the per-pixel spectral similarity, which was established by an unsupervised clustering algorithm (ISO-DATA) (Tou and Gonzalez 1974) and on the other by the context relationship of the different stream lines (Fig. 2). The context relationship was important to reduce the spectral variations produced from shallow-water zones. Shallow-water regions with great quantities of macrophyte beds filtered the incoming flows and significantly affected the spectral responses. Other features, like artificial rock islands (i.e., St. Lawrence Seaway structures), also affected the spectral information of the water masses. All of these features introduce specific stream line patterns. The individual stream lines were, however, easily linked to the principal flow of the different water masses. The rock islands, macrophyte beds, and bottom sediment features could be identified on all images and became helpful

Table 1. Station number assignments with respect to time and water mass distribution (see Fig. 1).

Main zones	Contributing water mass	Transect within Lac Saint-Pierre		
		Upstream	Middle	Downstream
6 Jun 01				
North zone	Northwest tributaries*	—†	—	—
	Ottawa	7,8,9	10,11,12	25,26
Central zone	St. Lawrence (Great Lakes)	5,5b,6	13,14‡	23‡
South zone	Richelieu/Yamaska/Saint-François	4	15	—
	Saint-François	0,1,2,3‡	16,17,18	22,‡22x‡
27 Jun 01				
North zone	Northwest tributaries	9	—	—
	Ottawa	7,8	12	25,26
Central zone	St. Lawrence (Great Lakes)	4,5,6	13,14‡	23,‡24‡
South zone	Richelieu/Yamaska/Saint-François	2,3	15,16	22,‡22x
	Saint-François	1‡	17,‡18	20,21
18 Jul 01				
North zone	Northwest tributaries	7,8,9	11	25,26
	Ottawa	—	12	—
Central zone	St. Lawrence (Great Lakes)	4,5,6	13	23,‡24
South zone	Richelieu/Yamaska/Saint-François	2,3	—	—
	Saint-François	1	14,15,16,17,18	20,‡21,‡22‡
13 Aug 01				
North zone	Northwest tributaries	7,8,9	11	25
	Ottawa	—	12	—
Central zone	St. Lawrence (Great Lakes)	4,5,6	13	23,‡24
South zone	Richelieu/Yamaska/Saint-François	1,‡2,‡3‡	15	22
	Saint-François	—	16	—

* Northwest tributaries is comprised of flows from the Maskinongé River and small tributaries from Sorel Island.
† Stations were either not in the correct position or could not be unequivocally assigned to a particular water mass.
‡ Predominantly in the water mass indicated but slightly intermixed with or adjacent to another water mass.

features to link similar spectral patterns among the images. This last point permitted us to take advantage of the finer spatial resolution (15 m) ASTER images to discriminate more conspicuous spectral features on the ETM images (30-m spatial resolution). The multidate link also helped us at times when thin cloud cover partly interfered with the water spectral information at certain locations in the image.

The different spectral classes, produced with the clustering algorithm on the red and green bands, were used to identify the specific lateral limits of the water masses (Fig. 2). These limits were used to confirm the distribution of the different stream lines in Lac Saint-Pierre. Although the water masses might evolve bio-optically from the upstream to the downstream portion of Lac Saint-Pierre (Fig. 1), the stream line continuity, evident on all images and delineating each of the water masses or components thereof, is clear. The stream lines are used to associate the upstream portion of each water mass with its downstream components. This approach permitted us to manually delineate each of the water masses on each satellite image.

Lac Saint-Pierre certainly has very shallow areas (<2 m, mostly in the southeast), wherein reflection off the bottom and the water might be confused in the green band, thereby confounding our interpretation of the water mass limits. We avoided this potential difficulty by restricting our analyses to areas in which the water depth was >2 m. Furthermore, in lakes like Lac Saint-Pierre, where significant amounts of suspended inorganic matter are present, spectral band absorption and reflection, particularly in the red band, will be mostly accounted for by the inherent properties of the upper 2 m of the water column.

By design, we tried to locate sampling stations in each of the water masses; however, this was complicated by the seasonal changes in the spatial distributions of the water masses. Hence, the assignment of particular sampling station numbers to a particular water mass was not always consistent during the sampling campaign (Fig. 1; Table 1).

In general, the northern zone is characterized by opaque and brown-colored water that is rich in suspended particles and relatively high in dissolved organic carbon (DOC) concentrations derived from humic and fulvic acids originating from podzoils of the northern watersheds (Bobée et al. 1977; Primeau 1996). It is influenced by waters coming mainly from Ottawa River and the Du Loup and Maskinongé Rivers. The central water zone, which includes the maritime shipping channel, is composed of transparent green-colored water originating from the St. Lawrence (Great Lakes) system and is characterized by relatively low DOC and suspended particle concentrations (Cossa et al. 1998). The maritime channel is the only prominent deep zone (average 12 m deep and ~245 m wide) in the lake. The southern zone is also brownish in color, but more transparent than the north zone water, and is characterized by relatively high DOC and low suspended particle concentrations.

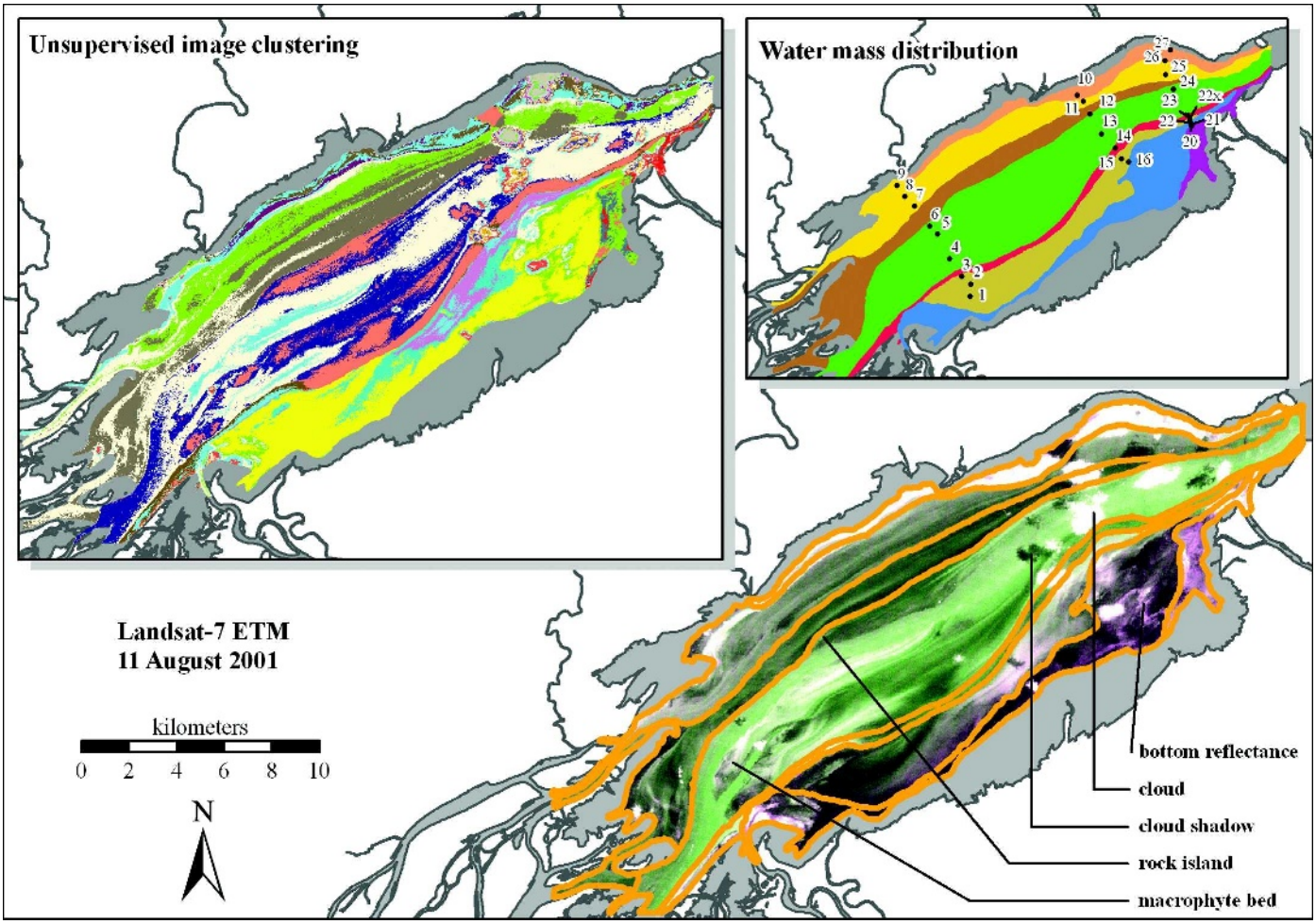

Fig. 2. Spectral delineation of the water masses for Lac Saint-Pierre (LSP) performed on Landsat-7 ETM images for 11 Aug 2001. This image is a color composite produced by enhancing the contribution of the green and red bands such that stream line patterns and other features are revealed. The insets show an unsupervised clustering image (left) and a water mass distribution map (right) for 11 Aug 2001.

We used the satellite image analyses to classify eight main water masses in the three main zones (north, central, and south) of Lac Saint-Pierre: three in the northern zone, one in the central zone, and four in the southern zone (Fig. 1; Table 1). The northern water mass comprised waters emanating from the (1) Du Loup and Yamachiche Rivers, (2) Maskinongé River and small tributaries emanating from the Sorel Island region that together we called the Northwest tributaries, and (3) Ottawa River. The central zone consisted of water arising from the St. Lawrence River (Great Lakes). The southern water zone was further parsed into the following water masses: (1) a mixture of Richelieu and Yamaska River waters, (2) a mixture of Richelieu, Yamaska, and Saint-François River waters, (3) Saint-François River water, and (4) water from the Nicolet River and several small tributaries that we here collectively refer to as the Southeast tributaries.

To highlight the effects of hydrodynamics on the longitudinal patterns in chemical and optical parameters, we focused much of our analyses (Table 1) on the water masses that provided the best data on longitudinal changes in these parameters (i.e., the Northwest tributaries, Ottawa, St. Lawrence (Great Lakes), Richelieu/Yamaska/Saint-François, and Saint-François water masses).

Determining transport times within each water mass—Current velocity and water levels were calculated with a two-dimensional (horizontal) HYDROSIM hydrodynamic model (Heniche et al. 1999), which uses a discretization of the shallow-water equations solved by the finite elements method. The model uses the conservative form of the quantity of movement from the Saint-Venant equations and takes into account spatial patterns of friction associated with the local substratum. This hydrodynamic simulation is similar to that of Morin et al. (2000*a,b*), with inflows at the upper boundary and an imposed water level at the downstream boundary. The finite element mesh used comprises a total of 80,000 elements and 114,000 nodes and covers the entire area from Montréal to Trois-Rivières (located immediately downstream of Lac Saint-Pierre). The inflows considered in this model correspond to discharges of the major tributaries on each of the sampling dates

Table 2. Discharges, volumes, and surface areas of the main tributaries of Lac Saint-Pierre on the four sampling dates. Discharge values are given for stations located near the mouth of the respective tributaries.

Tributary*	Discharge ($m^3 s^{-1}$)	Volume (km^3)	% total volume	Area (km^2)	% total area
08 Jun 01					
Great Lakes	7,427.0	0.574	63.78	117.85	37.75
Ottawa	1,369.0	0.166	18.40	64.65	20.71
Richelieu	547.8	0.062	6.84	24.51	7.85
St-François	331.8	0.078	8.64	76.18	24.40
Other	60.0	0.021	2.33	28.98	9.28
Total		0.900	100.00	312.17	100.00
27 Jun 01					
Great Lakes	6,753.0	0.519	69.39	119.73	41.82
Ottawa	903.6	0.126	16.89	57.45	20.07
Richelieu	408.1	0.057	7.59	29.37	10.26
St-François	62.0	0.032	4.33	47.46	16.58
Other	44.7	0.014	1.81	32.29	11.28
Total		0.747	100.00	286.30	100.00
18 Jul 01					
Great Lakes	6,746.0	0.523	70.92	118.45	43.14
Ottawa	780.7	0.107	14.46	54.40	19.81
Richelieu	282.9	0.038	5.15	16.96	6.18
St-François	147.0	0.052	7.07	62.66	22.82
Other	67.9	0.018	2.40	22.09	8.05
Total		0.737	100.00	274.56	100.00
13 Aug 01					
Great Lakes	6,630.0	0.488	79.22	131.99	50.79
Ottawa	509.7	0.076	12.39	47.15	18.14
Richelieu	158.7	0.036	5.90	29.71	11.43
St-François	18.9	0.009	1.52	26.43	10.17
Other	13.6	0.006	0.97	24.61	9.47
Total		0.616	100.00	259.89	100.00

* Other, Yamaska, Maskinongé, and Du Loup Rivers.

(Table 2). Bottom friction was parameterized with the use of substratum maps, whereas friction from aquatic plants used in the hydrodynamic model changed spatially and temporally in relation to the seasonal growth of plants.

The stream line function is a well-known technique for visualizing a particle's path in a hydrodynamic field (Merzkirch 1974). Because the hydrodynamic simulations of Lac Saint-Pierre are at steady state, the stream line function can be used to estimate a particle's path and transport time between two points on the same line. Several stream lines joining two stations located on the same path were extracted and used to calculate the mean velocity and total distance traveled on the particle path. The total distance divided by mean velocity gives total transport time between two stations. This transport time was calculated for between five and eight discrete stream lines down the length of the lake, depending on the sampling date.

UV radiation, photosynthetically active radiation, beam attenuation, and temperature profiles—A spectroradiometer (Model PUV-2545, Biospherical Instruments) was used to measure the cosine-corrected downwelling underwater irradiance (E_d) at 313, 320, 340, 443, and 550 nm and downwelling cosine-corrected photosynthetically active radiation (PAR) at 400–700 nm. The PUV-2545 was equipped with a C-star transmissometer (Wet Labs Inc., 25-cm path length, λ = 488 nm) for measurement of underwater particle attenuation (scattering and absorption). The instruments were slowly lowered through the whole water column at each station, and at least 100 measurements m^{-1} were captured to a laptop computer. Light data were corrected by subtracting "dark irradiance" values (obtained when the instrument was fitted with a light-tight neoprene cap at in situ temperatures) from $E_d(\lambda)$ readings. Diffuse vertical attenuation coefficients (K_d) were calculated by linear regression of the natural logarithm of E_d versus depth. The depth to which 1% of subsurface irradiance penetrated ($Z_{1\%}$) was calculated as $4.605/K_d$ (Kirk 1994). Transmittance values (Tr) were converted into beam attenuation (C, cm^{-1}) with the formula

$$C = \frac{-1}{x} \ln(\mathrm{Tr})$$

where x is the path length (25 cm) of the light beam.

Within the photic zone, C at 0.4 m were calculated from smoothed values with a spline curve (JMP 4.0, SAS institute Inc.) from the relationship between C versus depth.

Mean temperatures, recorded simultaneously with the spectral data, were averaged from depth profiles conducted through the whole-water column. The water column was

generally well mixed and exhibited very little, if any, thermal stratification (data not shown).

Inorganic and organic dry weight—Duplicate subsurface (40-cm) water samples were filtered on previously combusted (450°C for 4 h) and weighed (0.1 mg precision, Mettler Toledo balance model AB104) 25-mm Millipore glass fiber filters (0.7 μm pore size) and were stored frozen (−20°C) for 2 to 6 months until analysis. Filters were then heated at 60°C for 24 h until dry and placed in a dessicator until they could be weighed. The filters were then combusted at 450°C for 16 h and weighed again.

Particulate organic carbon, CDOM, DOC, Chl a*, and absorbance coefficient measurements*—Particulate organic carbon (POC) determinations were made on duplicate subsurface (~40 cm) water samples filtered onto precombusted 25-mm Millipore glass fiber filters (0.7 μm pore size) and frozen (−20°C) until measured on a Perkin-Elmer CHN analyzer (Model 2400). CDOM and DOC samples were filtered through 0.22-μm rinsed Milli-Q Isopore membranes (Millipore) and stored in the dark at 4°C until analysis. CDOM absorption spectra were measured in 10-mm quartz cells at 1-nm intervals between 290 and 900 nm with a spectrophotometer (Shimadzu UV-2401PC) referenced against 0.22-μm–membrane filtered Milli-Q water. We used absorbance at 690 nm (where the temperature dependency is near zero) to correct the UV absorption values (Laurion et al. 2000). Absorbance values at 340 nm were converted to absorption coefficients (*a*CDOM) with the following equation.

$$a\mathrm{CDOM}\left(\mathrm{m}^{-1}\right) = \frac{2.303}{\mathrm{abs}_{340\ \mathrm{nm}} \cdot 0.01}$$

DOC was analyzed by high-temperature catalytic oxidation on a Dohrmann DC-190 Total Carbon Analyzer or a Shimadzu TOC 5000A instrument. Both instruments quantify CO_2 released by combustion with the use of a nondispersive infrared detector calibrated daily with potassium hydrogen phthalate ($C_8H_5O_4K$). Filtered water samples were acidified with 20% phosphoric acid and purged for 5 min with the instrument's carrier gas, zero air or oxygen, to remove dissolved inorganic carbon before DOC determination. Determinations were corrected daily with system blanks estimated by regressing the results of low-concentration standards (0, 2, 5 mg C L^{-1}) analyzed as samples against their "true" value. The system blank corrects for a combination of carbon sources internal to the instruments and also residual carbon in the reagent water used to make standards.

Chlorophyll *a* (Chl *a*) was measured after hot ethanol (8 mL at 70°C for 5 min) extraction (Nusch 1980). Extractions continued in the dark at 4°C for 1 h, after which absorbance was measured at 665 and 750 nm (Shimadzu spectrophotometer, UV-Probe) before and after acidification to correct for pheopigments.

For the particulate absorption coefficient (a_p), duplicate water samples were vacuum filtered through a 25-mm GF/F filter (Whatman) then stored in the dark at −80°C until analysis. Absorbance was measured every nanometer from 320 to 820 nm with a Shimadzu UV-2401 PC equipped with an integrating sphere (model ISR-2200). Absorbance values at 500 nm were converted to a_p by the quantitative filter technique (Roesler 1998).

Nutrients—Calcium, chloride, total dissolved nitrogen, NO_3^-, NO_2^-, dissolved silica, soluble reactive phosphorus, and total phosphorus concentrations were analysed according to standard methods in use at the National Laboratory for Environmental Testing in Burlington, Canada.

Numerical analysis—Multiple regression analysis was performed, with UVA attenuation (K_{d340}) as a dependant variable and CDOM, Chl *a*, POC, a_p, and inorganic dry weight as explanatory variables. The (squared) semipartial correlations were calculated with SYSTAT (SPSS Inc.) to express the unique contribution of the independent variables to the total variance of K_{d340}.

A discriminant analysis was used to calculate a linear discriminant function (Statistica 6.0, Statsoft Inc.) to predict which water mass a given sampling site belonged on the basis of its associated chemical, optical, or both characteristics. Before analysis, data were screened to ensure the assumption of similar dispersion of independent variables and were log transformed to satisfy the assumption of multivariate normality. Variables used in the final model were selected according to a stepwise backward procedure designed to minimize autocorrelation between independent variables.

Results

Spatial and temporal distribution of water masses—The relative distribution of water masses changed seasonally, mainly because of changes in the discharge of the four main tributaries relative to that of the St. Lawrence River (Fig. 1; Table 1). For example, the relative contribution (surface area and volume) of the Saint-François River diminished markedly, whereas the contribution of the St. Lawrence River (Great Lakes water) increased over time (Fig. 1; Table 1).

Water level fluctuations in Lac Saint-Pierre—Water levels in Lac Saint-Pierre are a function of discharge from the St. Lawrence River combined with discharges from its tributaries. During the summer of 2001, water levels were very low compared with the interannual mean (Fig. 1). For all sampling days, the level was 40, 60, and 80 cm lower than the interannual mean on 08 June, 27 June, 18 July, and 13 August, respectively. Such periods of low discharge are associated with a very low supply of water from the Great Lakes (Morin and Bouchard 2000).

Spatial and temporal heterogeneity in inherent optical and chemical characteristics—North–south patterns: The spatial patterns of some optical and chemical parameters across the middle transect of Lac Saint-Pierre are shown in Fig. 3. The middle transect was chosen because it most

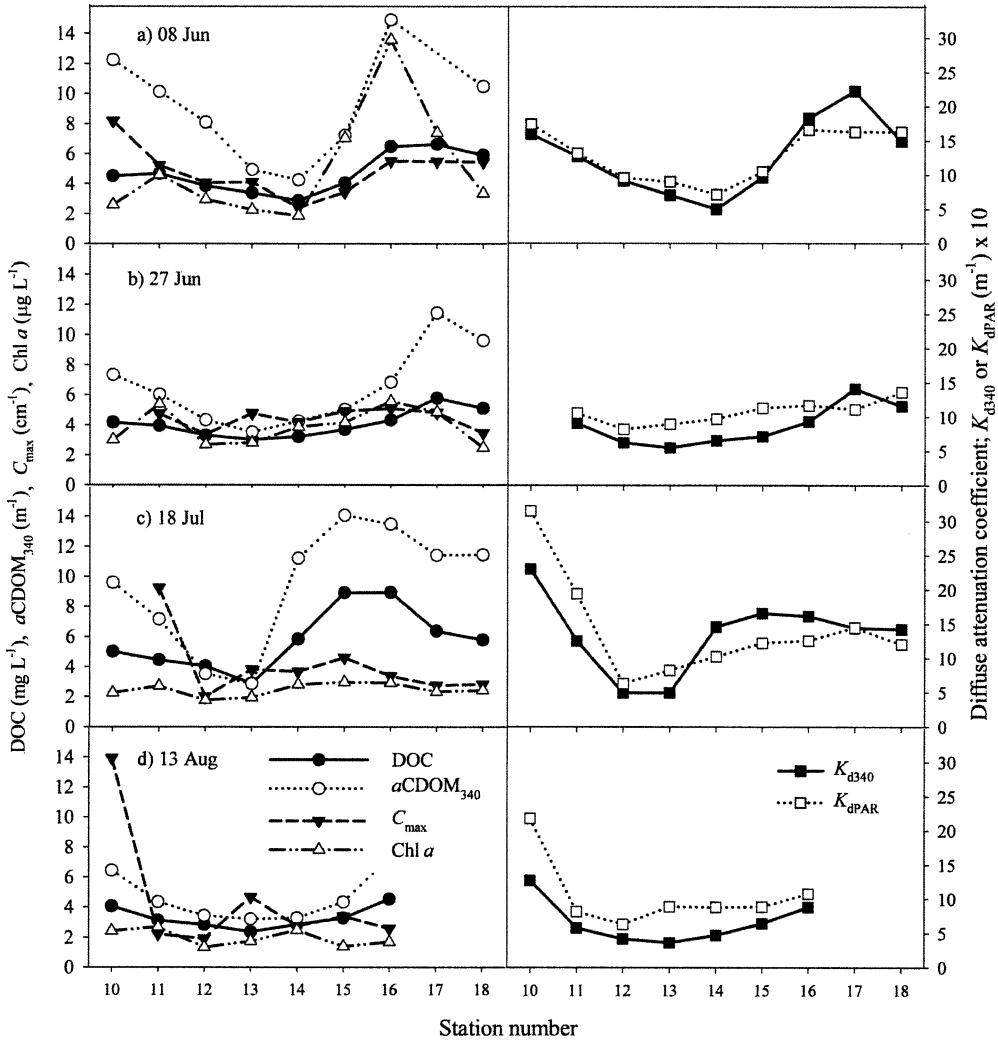

Fig. 3. Spatial variation in DOC concentrations, CDOM absorption coefficient (aC-DOM$_{340}$), maximum beam attenuation coefficient (C_{max}), Chl a concentrations, K_{d340}, and K_{dPAR} in sampling stations located in the midlake transect (see *Methods*) of Lac Saint-Pierre on (a) 08 Jun, (b) 27 Jun, (c) 18 Jul, and (d) 13 Aug 2001.

clearly demonstrates how the physical and chemical composition of incoming tributaries interact with within-lake processes to produce a complex and highly dynamic mosaic of underwater light climates in Lac Saint-Pierre. The penetration of UVA and PAR is highest in the St. Lawrence (Great Lakes) water mass and lower toward the north and south shores of the lake. These patterns in underwater light climate match spatial distributions of DOC and aCDOM$_{340}$ in the lake (Frenette et al. 2003).

Upstream–downstream patterns: Transport times (Figs. 4–6) in the main water masses in Lac Saint-Pierre ranged from 0.9 to 5.3 d (Northwest tributaries), 0.8 to 5.0 d (Ottawa River), 0.5 to 1.8 d (St. Lawrence), 0.7 to 3.5 d (Richelieu/Yamaska/Saint-François), and 0.3 to 5.6 d (Saint-François). Each water mass exhibited marked changes in its inherent optical and chemical properties in its passage down the lake (Figs. 4–6). These changes are most apparent in the Ottawa River and Saint-François River water masses, which demonstrated a general trend of increasing UV and PAR penetration downstream of the source tributaries (Fig. 4). Among the four sampling dates, there was no pronounced trend in K_{d313} or K_{d340} in the St. Lawrence River water mass; however, as with the Richelieu/Yamaska/Saint-François Rivers water mass, PAR attenuation decreased abruptly when the St. Lawrence River water first entered Lac Saint-Pierre (Fig. 4).

Not surprisingly, upstream–downstream patterns in DOC and aCDOM$_{340}$ were similar within each water mass (Fig. 5). However, each water mass also exhibited its own unique downstream pattern in relative loss or gain of DOC and aCDOM$_{340}$. For example, in the Saint-François water mass, both variables generally decreased downstream, whereas in the Richelieu/Yamaska/Saint-François water mass, they increased in the 08 June sampling period. There was little fluctuation in either variable in the St. Lawrence water mass. DOC and, correspondingly, aCDOM$_{340}$ values were generally lowest at the end of summer in all of the water masses. The a_p in the Saint-François, St. Lawrence, and Ottawa water masses followed a similar pattern to DOC and aCDOM$_{340}$ (Fig. 5). In general, a_p decreased

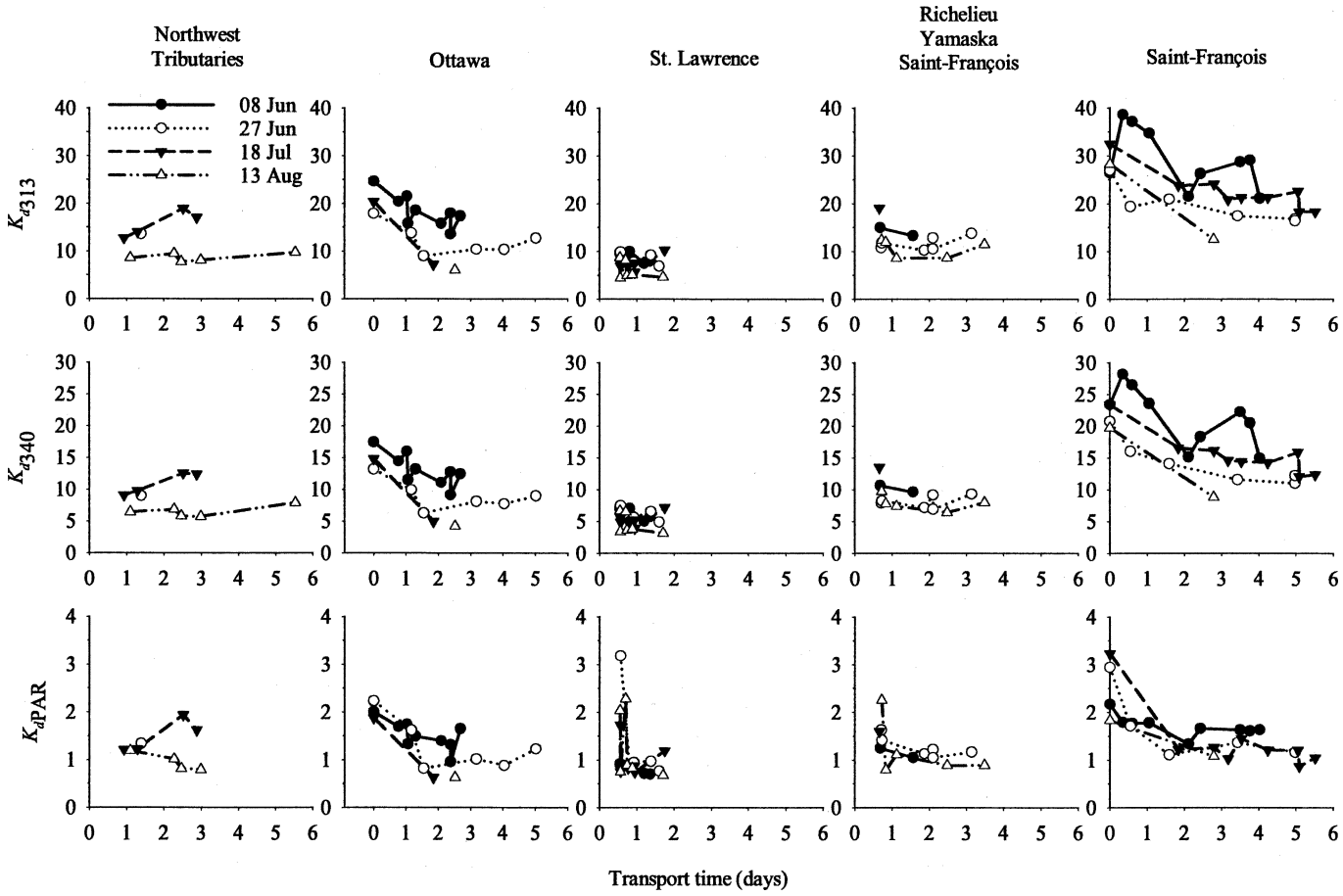

Fig. 4. Diffuse attenuation coefficients (K_d) for UVB (313 nm), UVA (340 nm), and PAR (400–700 nm) in five different water masses of Lac Saint-Pierre as a function of transport time on four dates in 2001; 08 Jun, 27 Jun, 18 Jul, and 13 Aug.

rapidly after the various tributaries entered the lake and then decreased more slowly, suggesting that particles were progressively settling downstream (Fig. 5).

The load of inorganic material was highest during the first sampling campaign after spring runoff, even in the rapidly flowing St. Lawrence water mass (Fig. 6). Chl *a* concentrations in the Saint-François water mass were highest and most variable during the first sampling period (Fig. 6). In subsequent periods, Chl *a* was either relatively constant or declined slowly downstream. POC concentrations generally declined downstream in all water masses (Fig. 6).

Multiple regression analyses with the use of all stations in all water masses revealed that most of the variation in K_{d340} was attributable to *a*CDOM on all sampling dates (Fig. 7). However, after 08 June, the contribution of particulate material to light attenuation increased significantly (from 0.5% to 24.8%) until the end of the season. On 27 June, both Chl *a* and especially inorganic dry weight explained 26.1% of the variance in UV attenuation. Later in the season, Chl *a*, absorbance because of particulate matter, and inorganic dry weight contributed to the explained variance 2.4%, 15.6%, and 24.8%, respectively.

The discriminant linear function (Wilk's lambda = 0.51; $p < 0.001$) used to reclassify the sampling site to the water mass to which they belonged had an overall success of 85%, with the greatest success for the Northwest tributaries (100%), the Great Lakes (95%), and the Saint-François River (100%) water masses (Fig. 8). However, it failed at predicting which stations belonged to the Ottawa and Richelieu Rivers (success rates of 20% and 67%, respectively). The variable $a\text{CDOM}_{340}$ allowed the greatest discrimination between water masses, but the overall model also relied on the contribution of total dissolved nitrogen, total phosphorus, and chloride concentrations (Table 3).

Discussion

Lac Saint-Pierre, as a representative of fluvial lakes, is physically very heterogeneous and represents a mosaic of habitats strongly connected to wetlands and upstream processes of the main river network and tributaries at various spatial and temporal scales. The spatial heterogeneity or physical complexity will be described mainly in terms of bio-optical and chemical characteristics in relation to transport time derived from hydrodynamic simulations.

Fluvial lake ecosystems: A mosaic of transport times and ages—One distinguishing feature of fluvial lakes is the general reduction in water velocity as each water mass enters the shallow depths and wider areas (greater volume)

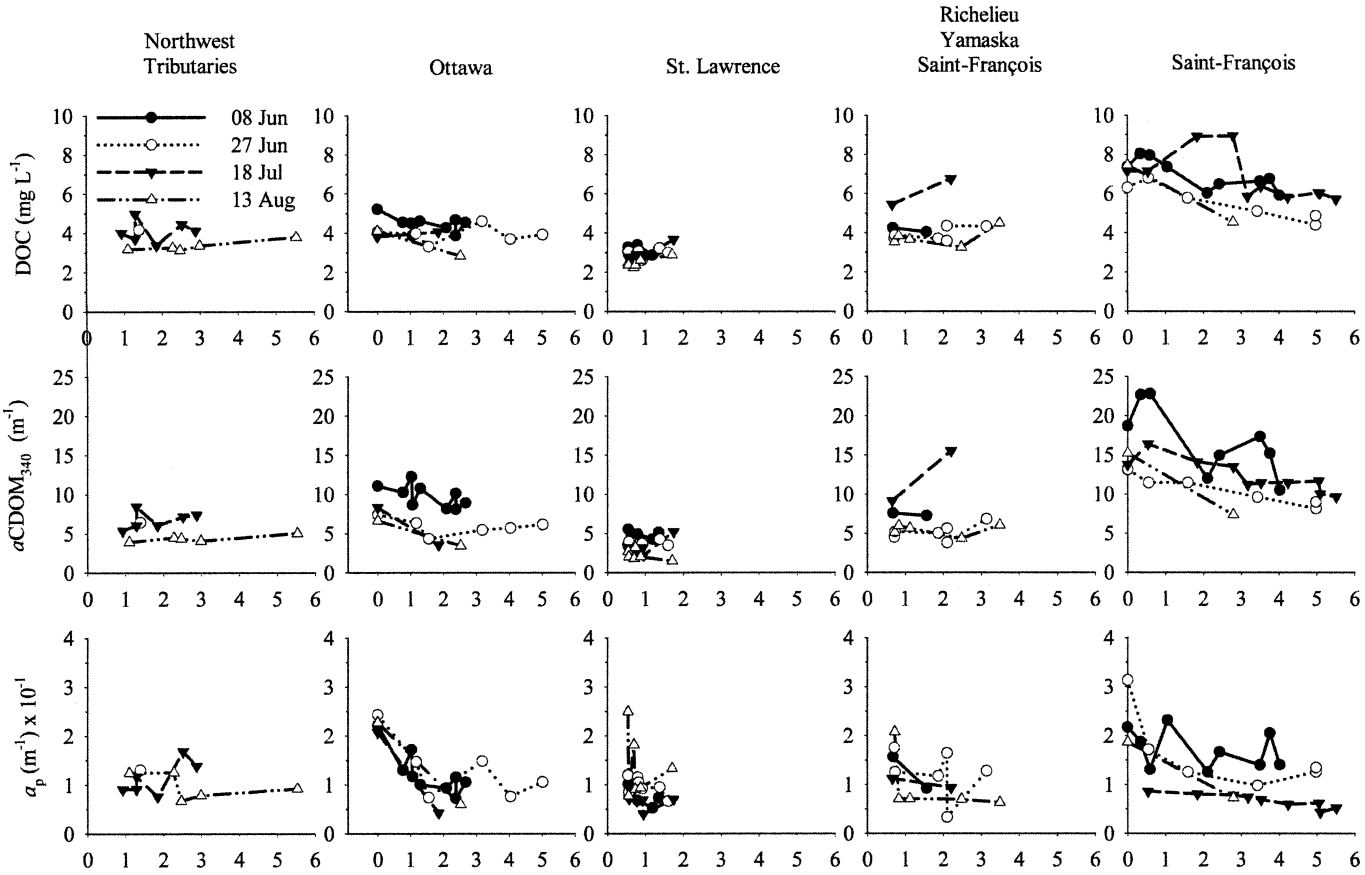

Fig. 5. DOC, $a\mathrm{CDOM}_{340}$, and the absorbance due to particulate matter (a_p) in the five different water masses of Lac Saint-Pierre as a function of transport time in 2001.

of fluvial lakes. This results in an increase in residence time of the various water masses within the lake. Longer residence times are generally associated with more complex food webs, higher biodiversity, and higher productivity (Lucas et al. 1999). An important point is that such increases occur differentially for each water mass, depending on basin morphology within the fluvial lake as well as discharge rates of each incoming tributary.

Differences in residence times affect the time a particular water parcel, and the particles it contains, spends in the lake before being swept back into the St. Lawrence River at the downstream end of the lake (Monsen et al. 2002). The physicochemical characteristics of the water masses are further modified by seasonally shifting patterns in macrophyte density and species composition, which are superimposed over the main downstream flow patterns. Changes in water level also strongly affect residence time within each water mass and, by implication, connectivity on the vertical dimension (e.g., Fig. 1; Table 1) and greatly influence the general deceleration of all water masses entering Lac Saint-Pierre, especially for those water masses distributed in the nearshore areas of the lake (i.e., Northwest tributaries, Du Loup/Yamachiche, and Saint-François water masses). This effect is most pronounced in the southern portions of Lac Saint-Pierre, a region that also corresponds to the area of highest biological productivity. Every lateral (north–south) transect across the lake is thus a mixture of water masses with different ages and origins (i.e., different tributaries) and temperatures. These differentially aging water masses are further influenced by within-lake processes downstream.

A mosaic of underwater light habitats—Our analysis of spectral components of the different water masses integrates the effects of seasonal changes in water levels and related changes in light-attenuating chemicals (e.g., CDOM) and suspended particles. CDOM explained most of the UV attenuation and allowed the greatest discrimination between water masses. It highlights the large spectral heterogeneity in underwater conditions that can be encountered in fluvial lakes and showcases the utility of bio-optical approaches in quantifying the magnitude of site-to-site variation in all dimensions.

North–south axis (transverse variability)—Seasonal changes in water levels influenced the distribution of water masses through the reduced contribution in area and volume of nearshore waters of the Saint-François and Ottawa River water masses (Fig. 1a–d). This had the effect of increasing the relative contribution of St. Lawrence–derived water later in the summer. These lateral changes in connectivity of the water masses with wetlands influenced

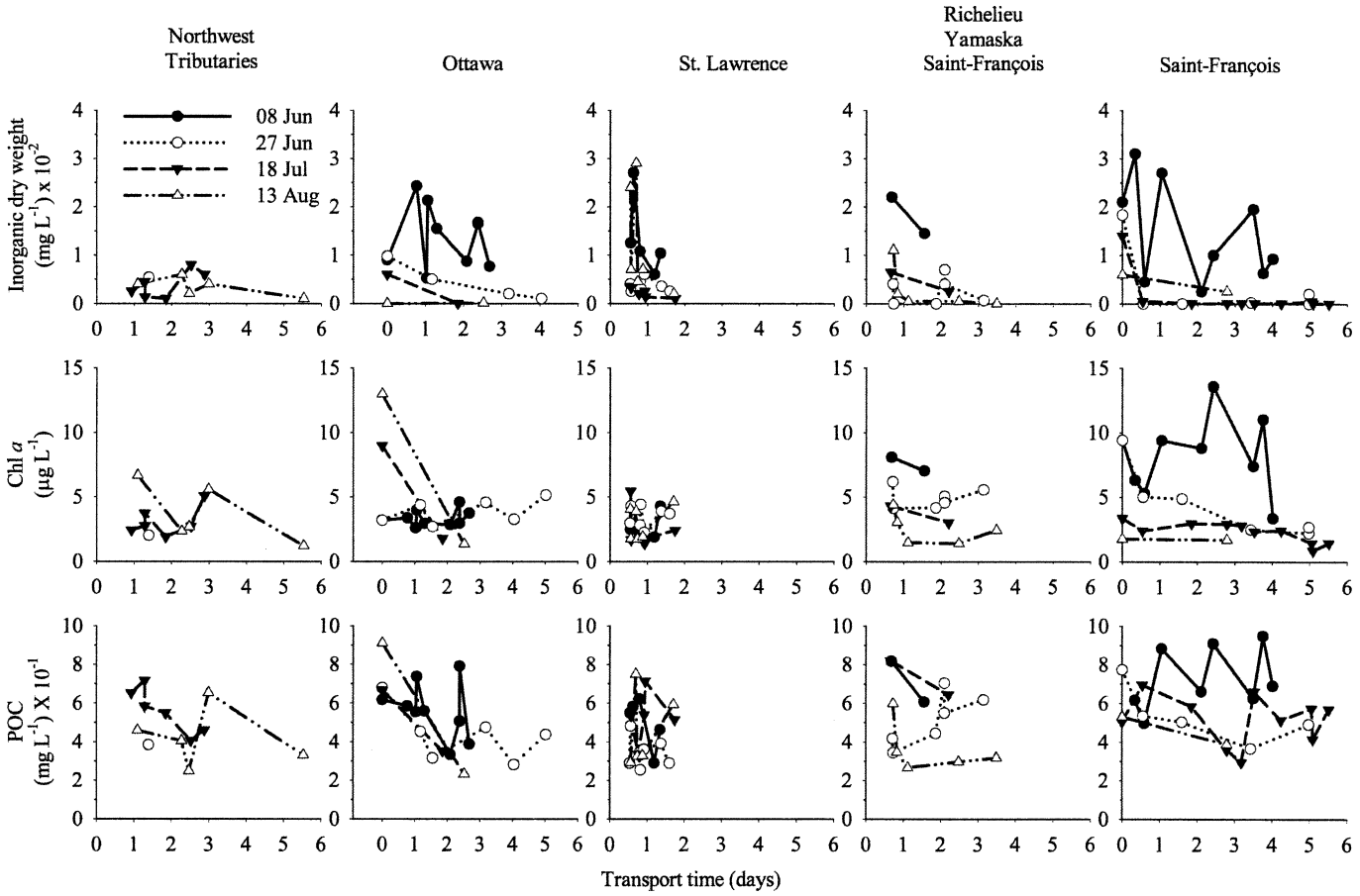

Fig. 6. Sestonic inorganic dry weight, Chl *a*, and particulate organic carbon (POC) in the five different water masses of Lac Saint-Pierre as a function of transport time in 2001.

the magnitude of matter transfers (e.g., CDOM and particulates), which affected light attenuation.

Upstream–downstream axis (longitudinal variability)—The water masses are further modified downstream, resulting in changes to their spectral signatures as a direct function of transport time. For instance, water masses originating from the slower moving St.-François and Ottawa River water masses show increased PAR and UV penetration downstream, whereas changes in the fast-moving St. Lawrence Great Lakes waters are less dramatic.

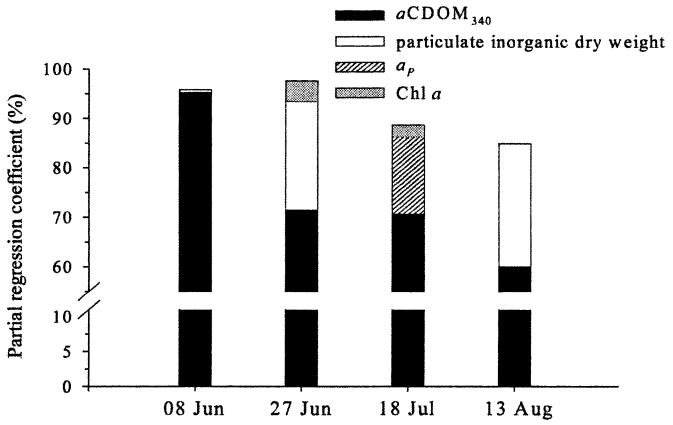

Fig. 7. Correlation coefficients (adjusted R^2) from each of the final variables selected by forward stepwise regression analyses for the four cruise dates in 2001.

This bio-optical variability within nearshore waters can be explained, in part, by the longer residence time, which provides more time for UV and microbial degradation processes to operate on DOC. The UV-exposed portions occupy a large percentage of the water column depending on location and time of the year (range = 7.1% to 100%, mean = 36.2%; Figs. 1, 3–5). UV photochemical (oxidative) reactions and microbial processes might increase UV radiation penetration in the water column because of photobleaching of allochthonous CDOM (Gibson et al. 2000; Osburn et al. 2001) and bacterial production of autotrophic DOM by degradation of recalcitrant CDOM (Wetzel et al. 1995; Osburn et al. 2001). For example, sampling along a 5-km longitudinal gradient in the Saint-François River water mass revealed a downstream decrease in the CDOM/DOC ratio, revealing a structural change in the DOM pool during a 9-h segment of the 3–5-d transit of the water mass through Lac Saint-Pierre (Martin et al. 2005). Such changes in inherent and emergent properties were not observed in the St. Lawrence water mass. This can

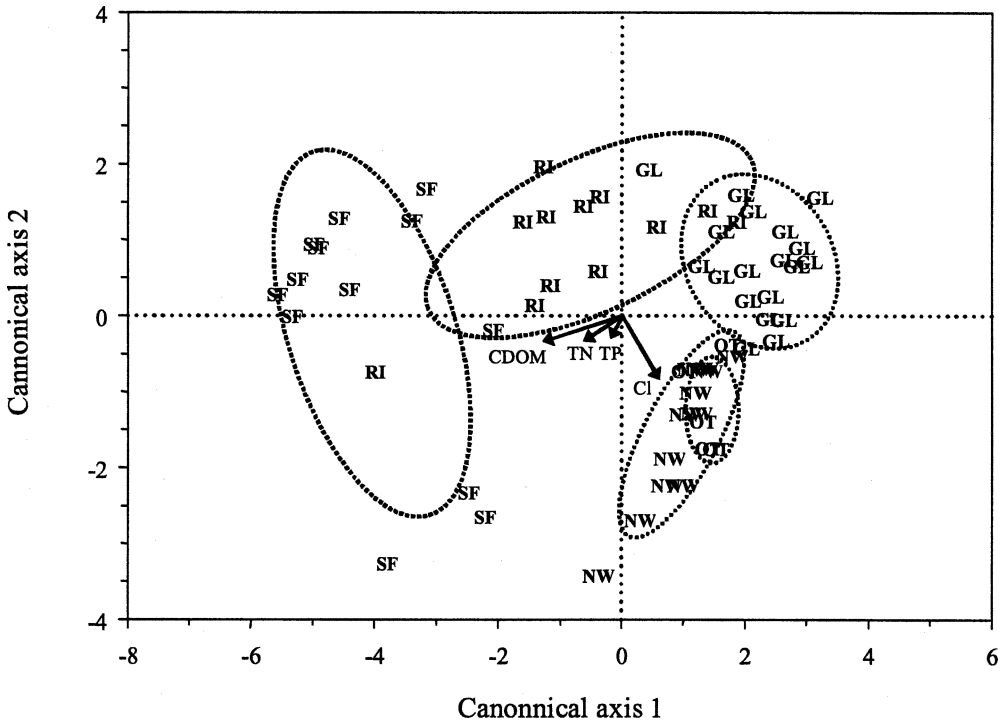

Fig. 8. Canonical representation of the five water masses and the four independent variables used in the linear discriminant analysis. Ellipses are centered on the mean of each group; their projection on the x and y axes are proportional to the range of the group. OT, Ottawa River water mass; NW, Northwest tributaries water mass; GL, Great Lakes water mass, RI, Richelieu River water mass; SF, Saint-François River water mass; CDOM, absorption coefficient of chromophoric dissolved organic matter at 340 nm; TDN, total dissolved nitrogen; TP, total phosphorus; Cl, chloride (Cl^-).

be explained by the (1) high transport times of this water mass in Lac Saint-Pierre, (2) the relatively old age of the source water (residence time of water in Lake Ontario is ~6 yr), and (3) minimal lateral mixing with adjacent water masses. Thus, the Great Lakes portion of the St. Lawrence water mass is one that has been affected by long-term exposure to UV and microbial degradation of DOC long before it enters Lac Saint-Pierre.

Connectivity in fluvial lakes—Our results demonstrate that the spatially and temporally complex nature of optical and chemical properties in fluvial Lac Saint-Pierre are a result, in large part, of their connectivity with inflowing tributaries and wetlands. Lac Saint-Pierre is thus very distinct from other shallow (nonfluvial) lakes because it is strongly influenced by upstream watershed processes that impose a strong directionality on the system. Inflowing tributaries inject subsidies with high amounts of nutrients, DOM, and particulate matter into the lake, part of which is strongly influenced by terrestrial exchanges (e.g., CDOM). These subsidies add to the pool of local (in situ) C and nutrients released from wetlands. In situ transformation and resulting characteristics of dissolved and particulate matter vary directly with transport time of each water

Table 3. Independent variables and statistical description of the linear discriminant analysis used to predict the water mass to which each sampling station belongs. SQ, square root.

					Correlation with canonical axis		
Model descriptors	Partial λ	Tolerance	F	p	1	2	3
SQ aCDOM	0.16	0.53	67.83	<0.001	−0.69	−0.35	0.20
SQ TDN	0.75	0.68	4.36	0.004	0.07	−0.21	0.06
SQ TP	0.69	0.83	6.09	<0.001	0.05	−0.05	−0.95
SQ Cl	0.40	0.78	19.89	<0.001	0.19	−0.89	0.22
				Eigenvalue	5.89	1.02	0.40
				Cumulative variance explained	0.81	0.94	1.00

mass. As a result, the underwater light environment shows a strong horizontal stratification (gradient) on both the lateral and longitudinal axis. The strong spatial and temporal variability in light characteristics and the rich nutrient environment contributes to the physical complexity and high productivity of Lac Saint-Pierre—factors which, we speculate, favor the high biodiversity characteristic of this lake.

Our study demonstrates that a critical, explicit analysis of both the horizontal and vertical dimension is a prerequisite to mapping the spatial heterogeneity in chemical and optical variables in fluvial lakes and, by implication, in other aquatic systems. Our study illustrates the promise of applying optical and physicochemical variables to construct habitat models that could ultimately be used to predict biodiversity and productivity in fluvial lakes and large rivers. It also clearly demonstrates that bio-optical instrumentation (e.g., spectroradiometers and fluorometers) for direct underwater and remote sensing applications (satellite reconnaissance) are promising tools to study spatial variability and physical complexity at various vertical and horizontal scales.

References

Bobée, B., F. Bordeleau, M. Cantin, and others. 1977. Évaluation du réseau de la qualité des eaux. Analyse et interprétation des données de la période 1967–1975. Ministère des Richesses naturelles, Direction générale des eaux. Vol. 2—Annexes, Q.E.-20.

Bruton, J. E., J. H. Jerome, and R. P. Bukata. 1988. Satellite observation of sediment transport patterns in the Lac Saint-Pierre region of the St-Lawrence river. Water Pollut. Res. J. Can. **23:** 243–252.

Bukata, R. P., J. H. Jerome, K. Y. Kondratyev, D. V. Pozdnyakov, and A. A. Kotykhov. 1997. Modelling the radiometric color of Inland Waters: Implications to a) Remote sensing and b) Limnological color scales. J. Great Lakes Res. **23:** 254–269.

Cossa, D., T.-T. Pham, B. Rondeau, B. Quémerais, S. Proulx, and C. Surette. 1998. Bilan massique des contaminants chimiques dans le fleuve Saint-Laurent. Environnement Canada —Région du Québec, Conservation de l'Environnement, Centre Saint-Laurent. Rapport scientifique et technique ST-163.

Frenette, J.-J., M. T. Arts, and J. Morin. 2003. Spectral gradients of downwelling light in a fluvial lake (Lake Saint-Pierre, St-Lawrence River). Aquat. Ecol. **37:** 77–85.

———, and W. F. Vincent. 2003. Bio-optical variability in the littoral zone: Local heterogeneity and implications for water quality monitoring, p. 41–59. *In* M. Kumagai and W. F. Vincent [eds.], Impacts of climate change on the world's freshwaters and estuaries: Global versus local perspectives on research and management. Springer-Verlag.

———, ———, and L. Legendre. 1998. Size-dependent C : N uptake by phytoplankton as a function of irradiance: Ecological implications. Limnol. Oceanogr. **43:** 1362–1368.

Frenette, M., C. Barbeau, and J. L. Verrette. 1989. Aspect quantitatifs, dynamiques et qualitatifs des sédiments du Saint-Laurent. Hydrotech.

Gibson, J. A. E., W. F. Vincent, and R. Pienitz. 2000. Hydrologic control and diurnal photobleaching of CDOM in a subarctic lake. Arch. Hydrobiol. **152:** 143–159.

Heniche, M., Y. Secretan, P. Boudreau, and M. Leclerc. 1999. A new finite element drying–wetting model for rivers and estuaries. Int. J. Adv. Wat. Resources. **38:** 163–172.

Huxel, G. R., and K. McCann. 1998. Food web stability: The influence of trophic flows across habitats. Am. Nat. **152:** 460–468.

Jerome, J. H., R. P. Bukata, P. H. Whitfield, and N. Rouseau. 1994. Colours of natural waters: 1. Factors controlling the dominant wavelength. Northwest Science **68:** 43–52.

Kirk, J. T. O. 1994. Light and Photosynthesis in Aquatic Ecosystems. 2nd ed. Cambridge University Press: United Kingdom.

Laurion, I., M. Ventura, J. Catalan, R. Psenner, and R. Sommaruga. 2000. Attenuation of ultraviolet radiation in mountain lakes: factors controlling the among- and within-lake variability. Limnol. Oceanogr. **45:** 1274–1288.

Lucas, L. V., J. R. Kosefs, S. G. Monismith, J. E. Cloern, and J. K. Thompson. 1999. Processes governing phytoplankon blooms in estuaries. II. The role of horizontal transport. Mar. Ecol. Prog. Ser. **187:** 17–30.

Martin, C., J.-J. Frenette, and J. Morin. 2005. Changes in the spectral and chemical properties of a water mass passing through extensive macrophyte beds in a large fluvial lake (Lake Saint-Pierre, Québec, Canada). Aquat. Sci. **67:** 196–209.

Merzkirch, W. 1974. Flow visualization. Academic Press.

Monsen, N. E., J. E. Cloern, L. V. Lucas, and S. G. Monismith. 2002. The use of flushing time, residence time, and age transport time scales. Limnol. Oceanogr. **47:** 1545–1553.

Morin, J., and A. Bouchard. 2000. Background information for the modeling of the Montréal/Trois-Rivières river reach. Scientific report SMC–Hydrométrie RS-100. Environment Canada, Sainte-Foy.

———, P. Boudreau, Y. Secretan, and M. Leclerc. 2000*a*. Pristine Lake Saint-François, St. Lawrence river: Hydrodynamic simulation & cumulative impact. J. Gt. Lakes Res. **26:** 384–401.

———, M. Leclerc, Y. Secretan, and P. Boudreau. 2000*b*. Integrated two-dimensional macrophytes-hydrodynamic modeling. J. Hydraul. Res. **38:** 163–172.

Nusch, E. A. 1980. Comparison of different methods for chlorophyll and phaeopigment determination. Arch. Hydrobiol. Beih. Ergeb. Limnol. **14:** 14–36.

Osburn, C. L., D. P. Morris, K. A. Thorp, and R. E. Moeller. 2001. Chemical and optical changes in freshwater dissolved organic matter exposed to solar radiation. Biogeochemistry **54:** 251–278.

Poole, G. C. 2002. Fluvial landscape ecology: Addressing uniqueness within the river discontinuum. Freshw. Biol. **47:** 641–660.

Primeau, S. 1996. Analyse de la qualité des eaux du bassin de la rivière des Outaouais, 1979–1994. Ministère de l'Environnement et de la Faune du Québec, Direction des écosystèmes aquatiques. Envirodoq EN960174, QE-105/1.

Rai, H., M. T. Arts, B. C. Wainman, N. Dockal, and H. J. Krambeck. 1997. Lipid production in natural phytoplankton communities in a small freshwater Baltic Lake; Schöhsee, Germany. Freshw. Biol. **38:** 581–590.

Roesler, C. S. 1998. Theoritical and experimental approaches to improve the accuracy of particulate absorption coefficients derived from the quantitative filter technique. Limnol. Oceanogr. **43:** 1649–1660.

Scheffer, M. 1998. Ecology of shallow lakes, p. 31–49. M. B. Usher, D. L. deAngelis, and B. F. J. Manly [eds.], Title of book. Chapman and Hall.

Sterner, R. W., and J. Elser. 2002. Ecological stoichiometry: The biology of elements from molecules to the biosphere. Princeton Univ. Press.

Tockner, K., F. Malard, and J. V. Ward. 2000. An extension of the flood pulse concept. Hydrol. Process. **14:** 2861–2883.

Tou, J. T., and R. C. Gonzalez. 1974. Pattern recognition principles. Addison-Wesley.

Ward, J. V., and K. Tockner. 2001. Biodiversity: Towards a unifying theme for river ecology. Freshw. Biol. **46:** 807–819.

Wetzel, R. G. 2001. Limnology: Lake and river ecosystems. Academic.

———, P. G. Hatcher, and T. S. Bianchi. 1995. Natural photolysis by ultraviolet irradiance of recalcitrant dissolved organic matter to simple substrates for rapid bacterial metabolism. Limnol. Oceanogr. **40:** 1369–1380.

Wiens, J. A. 2002. Riverine landscapes: Taking landscape ecology into the water. Freshw. Biol. **47:** 501–515.

Received: 16 November 2005
Accepted: 16 June 2006
Amended: 25 July 2006